Mechanisms of heterogeneous crystal growth in atomic systems: Insights from computer simulations

M. S. Gulam Razul,[a] J. G. Hendry, and P. G. Kusalik[b]
Department of Chemistry, Dalhousie University, Halifax, Nova Scotia B3H 4J3, Canada

(Received 14 June 2005; accepted 26 September 2005; published online 29 November 2005)

In this paper we analyze the atomic-level structure of solid/liquid interfaces of Lennard-Jones fcc systems. The 001, 011, and 111 faces are examined during steady-state growth and melting of these crystals. The mechanisms of crystallization and melting are explored using averaged configurations generated during these steady-state runs, where subsequent tagging and labeling of particles at the interface provide many insights into the detailed atomic behavior at the freezing and melting interfaces. The interfaces are generally found to be rough and we observe the structure of freezing and melting interfaces to be very similar. Large structural fluctuations with solidlike and liquidlike characteristics are apparent in both the freezing and melting interfaces. The behavior at the interface observed under either growth or melting conditions reflects a competition between ordering and disordering processes. In addition, we observe atom hopping that imparts liquidlike characteristics to the solid side of the interfaces for all three crystal faces. Solid order is observed to extend as rough, three-dimensional protuberances through the interface, particularly for the 001 and 011 faces. We are also able to reconcile our different measures for the interfacial width and address the onset of asymmetry in the growth rates at high rates of crystal growth/melting. © *2005 American Institute of Physics*. [DOI: 10.1063/1.2125688]

I. INTRODUCTION

The elucidation of the possible interfaces between the solid, liquid, and gas phases has certainly experienced many advances.[1–3] The solid/gas interface has been well characterized by experiments[4–6] and simulations;[7] its importance to technological applications has motivated much of the interest in understanding the solid/gas interface.[8,9] The liquid/gas interface has been successfully characterized by statistical mechanical theories[10] and generally serves as a basis for characterizing the other interfaces.[5] In contrast, the solid/liquid interface is not as experimentally accessible as other interfaces.[11] Experimental techniques such as transmission electron microscopy[12] (TEM) and synchrotron x-ray scattering techniques,[13] although very useful in probing the solid/liquid interface, are still limited to specific chemical environments and rather restricted applications.[14] Furthermore, the resolution of TEM under such conditions is still in the nanometer range, which is too coarse to characterize the molecular structure of all solid/liquid interfaces.[15] In order to complement experimental procedures and to provide better resolution of specific solid/liquid environments at the molecular scale, computer simulations have been proven to be effective.[16]

Computer simulations have provided important insights and detailed descriptions of solid/liquid interfaces.[15,17] These interfaces are obviously the regions where melting and freezing processes can occur. Yet, it is only after the position and structure of the interface have been characterized that detailed accounts of its role in freezing and melting can be understood. To this end, Burke *et al.*[18] first observed (in periodic boundary conditions) that the freezing interface of the 111 face-centered-cubic (fcc) system had in general no preference for either fcc or hexagonal-close-packed (hcp) stacking, with stacking faults occurring in about half the layers grown. A key observation was the presence of fcc and hcp lattice types that were suggested to be responsible for the slower growth of the 111 face. The clusters formed by these two lattice types within a given layer produced a mismatch that had to be annealed before real growth could occur. Burke *et al.*[18] also claimed that no such dual lattice structure was found for the 001 face. Another important conclusion of their simulation study was that during crystallization a layer grows by a "cooperative" motion of the atoms.

In characterizing the microscopic mechanisms of crystallization, Huitema *et al.*[19] have described the growth process of the 111 and 011 fcc faces as consisting of the ordering of the particles into the layers in front of the interface along with hopping of atoms from layers further away to layers closer to the interface. Consequently, the apparent density of the layers in front of the interface was observed to increase by about 10% on solidification. For the 001 face, no such increase in the apparent density of the layers was observed, although the distance between layers became smaller upon the ordering of the particles in the layers. Huitema *et al.*[19] concluded that this characteristic of 001 crystal growth provided a faster growth mechanism. While these descriptions of the crystal growth of atomic systems provide some insights, the microscopic mechanism of the crystallization and

[a]Present address: Department of Physics, St. Francis Xavier University, Antigonish, Nova Scotia B2G 2W5, Canada.
[b]Present address: Department of Chemistry, University of Calgary, 2500 University Drive N.W., Calgary, Alberta T2N 1N4, Canada. Electronic mail: peter.kusalik@ucalgary.ca

melting processes is still not completely clear. A systematic examination of these processes and their impact on the inherent interfacial structure have not been previously undertaken.

Other important properties of the solid/liquid interface, such as its interfacial free energy (or the interfacial tension), can be determined once detailed information on the nature of the interface is explored. Broughton and Gilmer[20] were among the first workers to calculate the interfacial free energy of the solid/liquid interface, and more recently examined by Davidchack and Laird[21] using a similar procedure. The former authors could not resolve differences in the interfacial free energies of the different crystal faces. However, Davidchack and Laird[21] have reported that the surface free energies (interfacial tensions) decrease in the order $001 > 011 > 111$. Their technique employs computer simulations to calculate a continuous thermodynamic path that can be integrated from a starting system of an independent bulk liquid and a bulk solid to a final state containing the interface. The methodology they employed, where planar cleaving walls were utilized as opposed to cleaving potentials to separate the phases, is a modified version of the procedure used by Broughton and Gilmer.[20] One of the important approximations of Davidchack and Laird[21] was to treat the interface as a planar entity, despite their own observation that the interface is generally "rough" on a short time scale. However, they justified this assumption by claiming that the fluctuations in the interfacial position should average out to a planar surface.

In a study by Morris and Song,[22] the order of interfacial free-energy differences matched those of Davidchack and Laird.[21] The method used by Morris and Song[22] examines the "fluctuations" in the height of the interface. Utilizing an order parameter to label particles as solid, liquid, and interfacial particles, this method then provides a reference point from which to calculate the height of the interface. This approach assumes the interface to be a line that can be used to demarcate solid from liquid and it is the deviations from this reference position that characterize the interface. The interfacial energy as defined in Morris and Song's study is the energy changes associated with such fluctuations; thus low interfacial energy is equated to smaller fluctuations.

In work by William *et al.*[23] using coupled Landau-Ginzburg equations based on a mean-field approximation of the fcc lattice gas with nearest- and next-nearest-neighbor interactions, the focus was on the relationship between particle interactions, packing geometries, and the intrinsic properties of the nonequilibrium interface, specifically on interfacial structure and interface mobilities. They found that the surface tension of the 001 face was lower than that of 111, and they also determined that the structural fluctuations of the 001 face are larger than those of 111. In addition, they identified the importance of the dynamics of interfacial transients manifested through the crystalline fluctuations in the liquid next to the solid.

The observations noted above suggest that fluctuations are an integral part of the equilibrium and nonequilibrium solid/liquid interfaces. In light of these observations, the claim that the interface is planar (at an instant in time at the molecular scale) is perhaps questionable. Moreover, descriptions of a dividing surface that separates a bulk solid and bulk liquid are unrealistic as it implies the *unique* existence of such a complex three-dimensional surface. The unambiguous classification of particles at this surface as solid or liquid remains very challenging.

In order to address some of the issues discussed above, Gulam Razul *et al.*[17] have provided an unambiguous means of characterizing the width and position of the solid/liquid interfaces of freezing and melting systems. They have shown that the 001 crystal face has a consistently larger value of the interfacial tension than the 111 face. This observation is in accord with the fact that the interfacial widths of 001 are always larger than those of the 111 face; in addition to being narrower, the latter interface appears to be smoother and exhibits smaller structural fluctuations. The values for interfacial tension and width of the 011 interface are intermediate between those of the 001 and 111 crystal faces. In addition, large structural fluctuations of the interface away from planarity were observed. The effective width of the interface therefore originates from the average local change of the order-parameter profile function (such as the energy or density) when moving from the bulk liquid to the solid, as well as fluctuation of the position of the interface relative to some frame of reference.[17] Most measurements of the interfacial widths fail to recognize the latter contribution to the effective width.[24–27]

The aim of the present work is to provide a clear description of the microscopic structure of the interface of an atomic system and to elucidate the mechanisms of crystallization and melting. Previously, Gulam Razul *et al.*[17] have employed nonequilibrium simulations to examine interfacial properties of growing fcc and bcc crystals; utilizing this new approach here will enable us to extract detailed descriptions of the freezing/melting interface. Our analysis will rely on both (moving frame) profile functions and detailed mechanistic discussions of the 001, 011, and 111 freezing/melting interfaces. Through a detailed analysis of layers coupled with specific tagging of particles we will show how the structural fluctuations contribute to crystal growth and the properties of the different crystal faces.

This paper is organized as follows. Section II briefly describes our simulation methodology that is used to generate nonequilibrium steady-state crystal growth conditions; it also provides some simulation details for the systems under investigation. Section III details the methods employed in our analysis of crystal growth/melting. In Sec. IV we present and discuss our results. Finally, Sec. V provides our concluding remarks.

II. METHODOLOGY

A. Steady-state simulations

Details of the present methodology for studying steady-state crystallization and melting have been presented elsewhere;[17] what follows is a brief overview of this approach. This novel methodology consists of two key aspects: the inclusion of localized thermostats and the movement of these thermostats (in a periodic system) to achieve steady-

state growth/melting. The heat source and heat sink (thermostats) are introduced into two localized regions of the simulation cell. Thus, heat is able to enter one part of the system while being removed from another part in an efficiently controlled manner. In addition, any latent heat generated (removed) by crystallization (melting) can be effectively removed (added) in these simulations. The presence of the thermal gradient, within the system, is central to the success of this simulation technique.

The second key aspect of this methodology involves moving the heat source and heat sink through the system, as desired. The simultaneous movement of the thermostats (at some sufficiently slow preset speed) can effectively force one face of the crystal to grow under nonequilibrium steady-state conditions. As is common in simulations, periodic boundary conditions are applied, enabling the movement of the thermostats to eventually cycle through the whole system multiple times. Consequently, a given particle could undergo several changes of state during any particular simulation run. The inclusion of the heat source and sink, together with the movement of these thermostats, generates solid and liquid phases that are in a continual state of flux. In this way, the freezing and melting processes can be effectively controlled and investigated.

B. Interfacial descriptions

To aid in the characterization of the freezing/melting crystal interface we make extensive use of averaged moving-frame profile functions. For the detection of crystalline order, a two-dimensional (2D) crystalline order parameter Σ is used,[17]

$$\Sigma(z) = e^{-(i\mathbf{k}_{2D}\cdot\mathbf{r}_{2D})}, \tag{1}$$

where $\mathbf{k}_{2D}$ is a two-dimensional wave-vector commensurate with the unit-cell structure and $\mathbf{r}_{2D}$ is the position vector (x,y) of the particle within the two-dimensional slice. This enables long-range order in the plane perpendicular to the z direction (the direction of crystal growth) to be quantified. The energy and Σ profiles, as shown in Figs. 1(a) and 1(b), respectively, are then used to define solid, liquid, and interface regions in a steady-state system. However, close inspection of the profiles in Fig. 1 reveals that the precise positions and widths of the two interfaces are still difficult to pinpoint. In our previous work[17] we have provided an approach that involved taking the derivative of an energy (or Σ) profile with respect to the z coordinate. In doing so two clear extrema, one peak, and one valley (but henceforth referred to as "peaks"), corresponding to each interface, are observed. Figures 1(a) and 1(b) show examples of this behavior. The derivative of the Σ order parameter [see Fig. 1(b)] exhibits similar peaks at the same positions to those evident in Fig. 1(a) for the derivative of the energy profile. This consistent behavior of the extrema, as seen in Fig. 1, enables identification of the positions of the freezing and melting interfaces; the width of the peaks can be understood to correspond to the interfacial width. Longer simulation runs (of more than 10^6 time steps) than those reported in our previous work[17] reveal

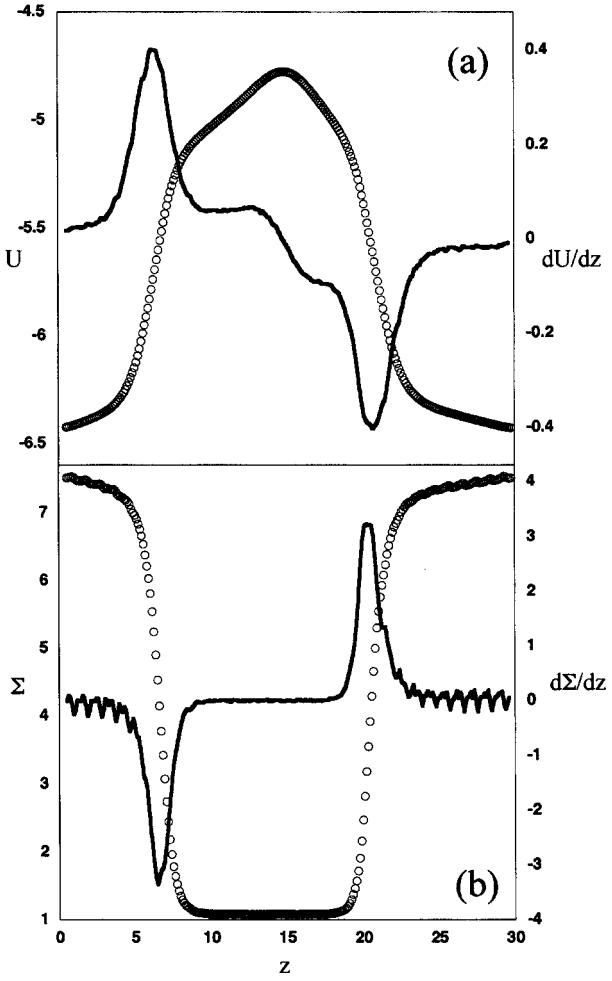

FIG. 1. (a) Energy and (b) structural order-parameter profiles, together with their derivatives with respect to z. The circles represent the original profile data, while the solid lines are their respective derivatives. The extrema in the derivatives correspond to the positions of the freezing and melting interfaces, while the widths of the peaks correspond to the interfacial widths. The system shown is a LJ 111 steady-state system with a moderate gradient and at a low velocity.

no changes in the profiles (or in atomic descriptions of the interface).

Additionally, the derivative of our energy function can be interpreted as an average force in the z direction experienced by a particle at that position in the system. Therefore, the extremum values for the melting and freezing interfaces can be immediately interpreted as the interfacial tension (or interfacial free energy). It has been previously observed[17] that the derivatives of the energy and Σ order-parameter profiles are sensitive measures of the changes occurring in the interfacial region.

C. Simulation details

In the present study the 001, 011, and 111 crystallographic faces of fcc crystals are examined for systems interacting with the Lennard-Jones (LJ) potential. The simulations described here are an extension of the set of simulations from Gulam Razul *et al.*[17] In the analysis below all quantities are given in the reduced units appropriate for the Lennard-Jones potential. System sizes (with box dimen-

sions) of 4320 ($13.17\sigma \times 11.87\sigma \times 30.26\sigma$), 4608 ($13.72\sigma \times 12.94\sigma \times 29.50\sigma$), and 4352 ($12.95\sigma \times 12.95\sigma \times 29.46\sigma$) particles for the 111, 011, and 001 crystal faces, respectively, were investigated. These systems were typically subjected to a moderate (0.2) temperature gradient and were studied at a moderate velocity (0.06). These conditions were chosen because they have been previously[17] shown to be well suited for the examination of the crystallization and melting behavior of LJ systems. Where appropriate, the results obtained for higher velocity and larger gradient systems (refer to Gulam Razul *et al.*[17]) will be discussed. Where comparisons were performed essentially no gradient dependence was observed in the properties of the interface, in agreement with our previous work.[17]

III. DETAILS OF ANALYSIS

A. Representative configurations

Analysis of system configurations will be a key component of the present study since one of its goals is to provide a systematic and consistent microscopic description of the mechanisms involved in crystallization and melting. In molecular-dynamics (MD) simulations, the many trajectories of all the particles of the system are followed in time, where at every time step their position will change. To facilitate viewing of the behavior important to the present study, an averaging procedure was required. The purpose of the averaging procedure was effectively to remove the thermal motion of the particles so that any net translational motion can be easily observed. This consequently allowed the characterization of the interfacial region and permitted atomic-level details of the freezing and melting processes under steady-state conditions to be examined. In our procedure this was accomplished by maintaining rolling averages of particle positions over 80 time steps and subsequently dumping these averaged coordinates (an averaged configuration) every 750 time steps. Typically, a sequence of a few hundred such configurations was produced. This optimum averaging procedure was selected based on the smallest time window and lowest frequency of dumps necessary to capture the essential physics of the system. For visualization purposes, the multiple files produced were then animated to view the time-dependent behavior of the particles in a single layer, as many layers, or as a whole system. For visualizing the microscopic behavior of the atoms during crystal growth and melting, we have used standard visualization software and have also developed and adapted software to facilitate visualization of the physical processes within the systems being investigated.

One means of elucidating the critical structural aspects of the interface was to superimpose the derivatives of the energy and Σ profile functions on a series of representative time-averaged configurations of the steady-state atomic system; an example is shown in Fig. 2. In this figure, the (averaged) atomic structure of the system is apparent as overlapping circles projected onto the *z*-*y* plane. This representation facilitates observation (and distinction) of the solidlike and the liquidlike regions. In this way, the structure of the crystallizing and melting interfaces has been probed. We have ascertained the degree of crystalline character through the

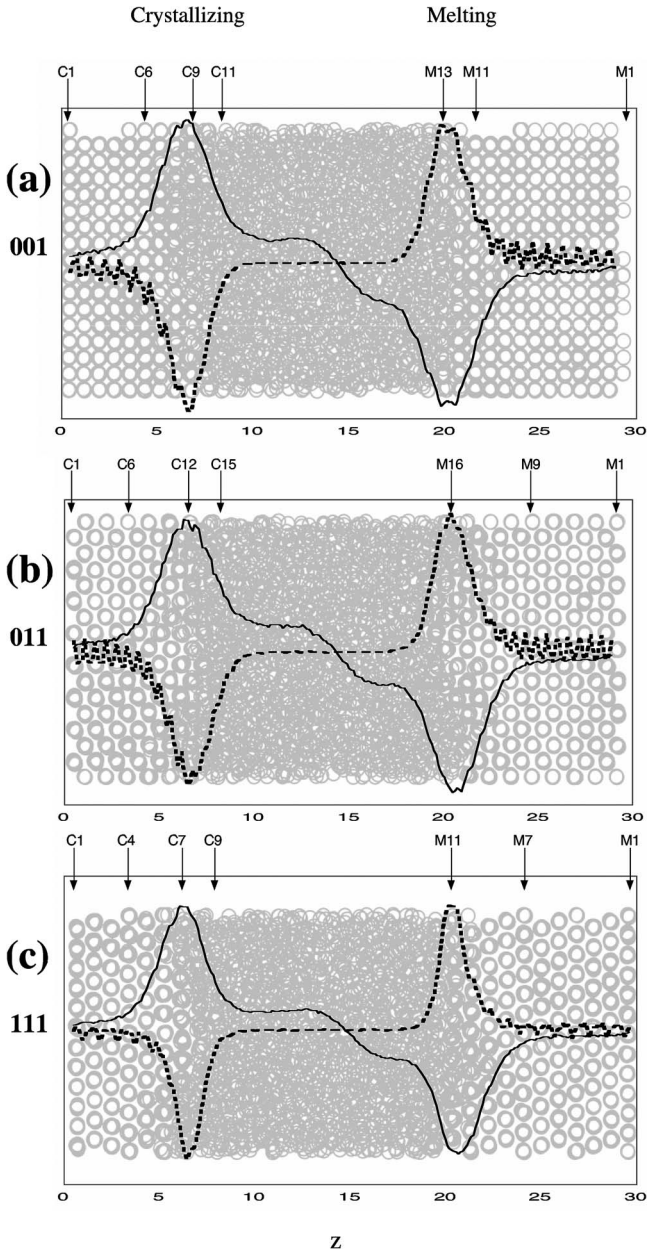

FIG. 2. Representative averaged configurations of 001 (a), 011 (b), and 111 (c) steady-state systems. Derivatives of the energy and Σ profiles for each system are superimposed as solid and dashed lines, respectively. The positions of the crystallizing and melting interfaces are as indicated for each system along with the layer numbers used in the discussions. The layers are labeled in ascending order from the solid to the liquid side for both interfaces.

interface and monitored the extent of structural fluctuations occurring at growing or melting fronts. Such sets of the averaged configurations also allow us to examine the nature of the fluctuations that can occur in an interface during steady-state growth or melting. They also provide important insights into the meaning of interfacial widths as defined by the derivatives of the energy and Σ profiles.

B. Slice identification and monitoring

In the analysis of the averaged configurations from our simulations, slicing of the "crystal" at the interface was performed in two ways. The first approach involved slicing the

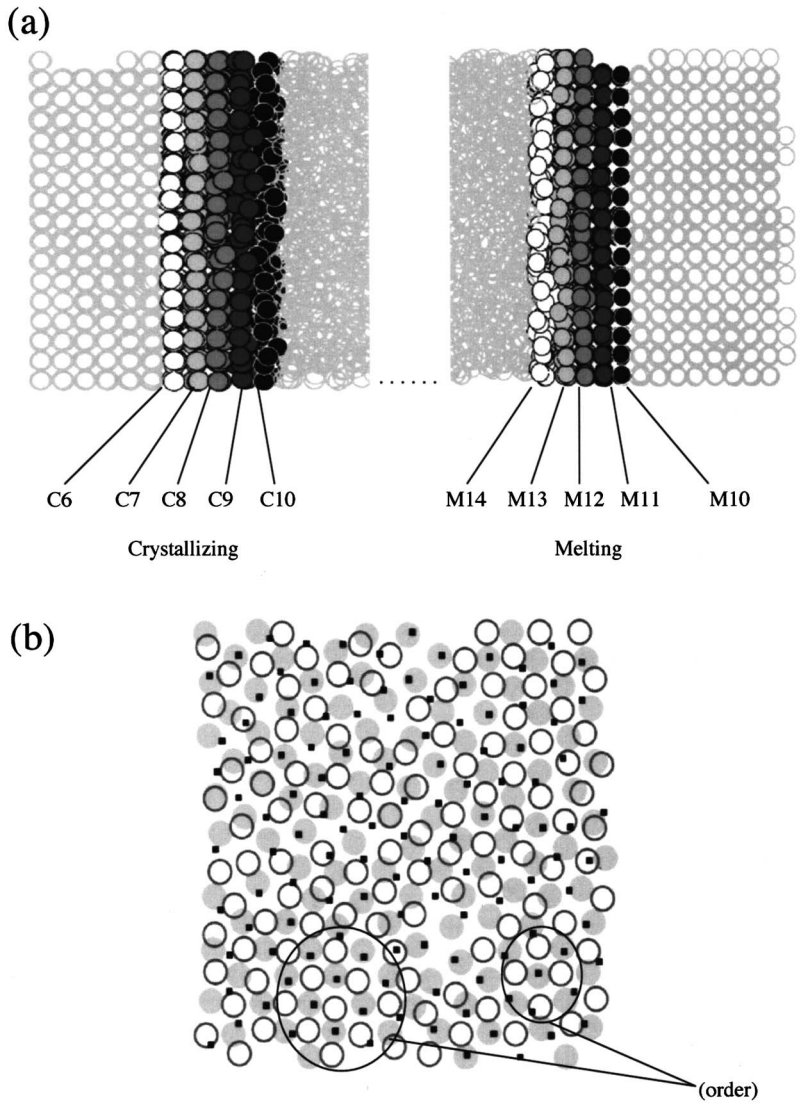

FIG. 3. (a) Layers of the crystallizing (C6–C10) and melting (M10–M14) interfaces of an averaged configuration of a LJ 001 fcc system. Five slices are identified and labeled (shaded differently) for each interface with the layer numbers as given in Fig. 2(a). (b) The forward view of three layers: C10 (small squares), C9 (open circles), and C8 (filled circles). Areas showing crystalline order have been identified.

system near the interface into layers as determined visually. These layers, or slices, were then inspected systematically to identify and label the atoms in a particular layer. The percentage of crystalline character present in slices through the interface is obtained from the corresponding values of the Σ order parameter at the appropriate position. The degree of crystalline character of a slice is then simply the percentage relative to the Σ value of the bulk solid for a particular system. It was also useful to superimpose two or three consecutive layers and visually check for possible correspondence of the order (crystallinity) within successive layers [for example, see Fig. 3(b)]. The interfacial layers that will be discussed in Sec. IV are labeled "C" for those at a crystallizing interface and "M" for a melting front, where their numbers indicate their positions relative to the solid side of the interface, as shown in Fig. 3(a). The labeling of slices for any particular system is consistent throughout this paper (for example, for the 001 system in Figs. 3–6).

An alternative method we have used in our analysis of the formation (or disappearance) of layers involved the indexing (or tagging) of particles. As an example, let us assume we have produced a set of averaged configurations from a particular segment of a system run. The final averaged configuration is examined and the particles that compose the layers of the crystal near the interface are indexed (tagged). For visual identification, the particles that compose each of these slices are labeled a different color. It is then possible to follow the behavior of the tagged particles throughout the full series of averaged configurations, thereby allowing us to monitor at the atomic level how the process of crystallization occurs. This method also affords us detailed insights into the way neighboring slices might influence the slice of interest. The analogous (inverse) labeling scheme was also employed at the melting interface.

The visualization of slices is performed in two ways. The first is to inspect (display) only the tagged particles from the simulation. This allows one to identify possible nucleation sites that may form during crystal growth and provides a detailed view of how these particles interact and form a layer. The second approach involves the examination of one or a few layers of the system where tagged and untagged atoms are colored appropriately. This procedure was adopted because the process of crystallization (and melting) involves the cooperative behavior of many atoms/molecules,[17–19] where there are considerable exchanges of particles between layers. In this way, we can ascertain how a layer forms and

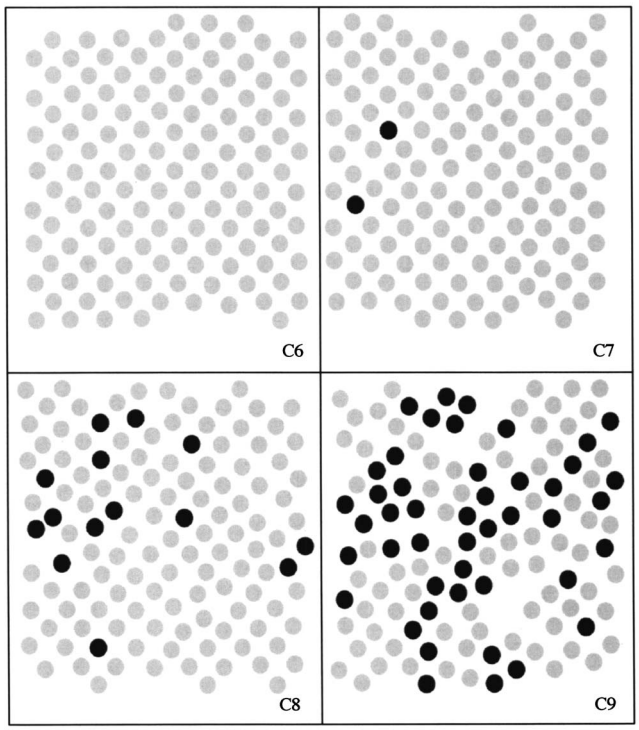

FIG. 4. Averaged configurations of four consecutive slices through the crystallizing interface of the LJ 001 fcc system. The layers are labeled as in Fig. 3. The dark atoms are transient particles as defined in the text.

how adjacent layers impact the crystallization of the layer of interest. Analogous analyses were performed on the melting interface.

We find that following a particular sliced layer through time during freezing/melting is essentially equivalent to simply inspecting the various slices of an averaged configuration of a particular interface; the various slices of any particular averaged configuration exhibit essentially the same stages that a specific slice goes through during the process of freezing/melting. For our subsequent discussions we will focus on the averaged configuration method (although both approaches were utilized in our investigation of the behavior). As an example, Fig. 4 shows four slices of a crystallizing interface, or alternatively, it can be viewed as different stages a slice would experience in forming a crystalline layer.

IV. RESULTS AND DISCUSSION

A. Interfacial structure of the 001, 011, and 111 crystals

To facilitate their identification, the various layers in a steady-state system have been uniquely labeled. For the 001 interface in the present study these are C6–C10 and M10–M14 for the crystallizing and melting interfaces, respectively, as shown in Fig. 3(a). The averaged configuration illustrated in Fig. 3 is representative of the 001 interface presented in Fig. 2(a). The structural fluctuations typical of the 001 interface are depicted in Fig. 5; a comparison of these three averaged configurations reveals that the 001 interface undergoes large structural changes during steady-state growth. Similar structural changes were also observed

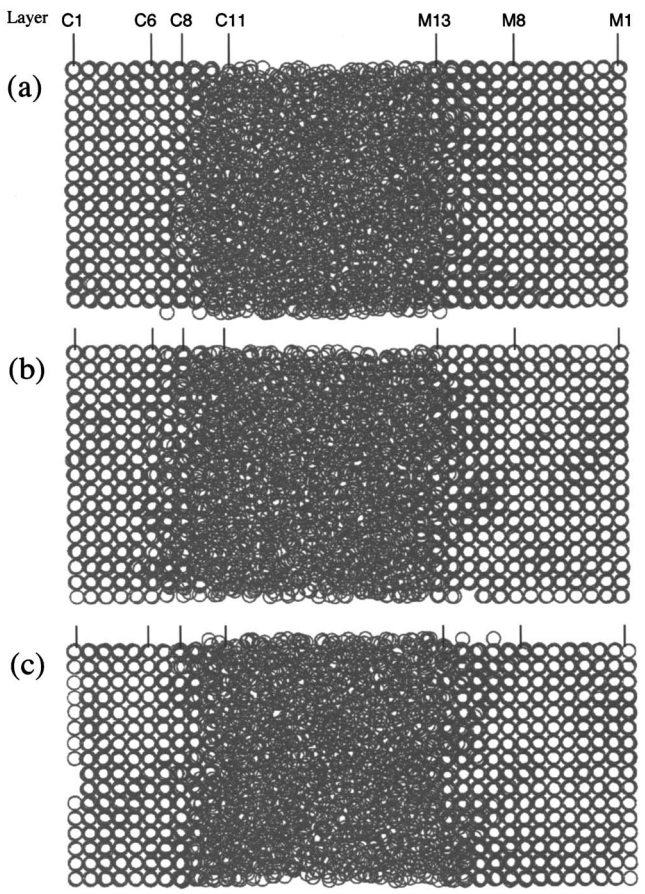

FIG. 5. Three averaged configurations of the LJ 001 fcc system depicted in the moving frame. The particles are shown as the open circles and the numbering of the layers are identical to Fig. 2(a); (a) represents an arbitrary initial frame 0, (b) frame 43, and (c) frame 50, where each frame is separated by 750 time steps.

by Moss and Harrowell.[28] It is clear that the structural fluctuations observed in Fig. 5 will contribute to the apparent thickness of the interface. Widths of 5.2σ (seven to eight atomic layers) and 4.2σ (five to six atomic layers) are observed for this interface if the derivatives of the energy and Σ profile functions are used, respectively.

We can apply a similar analysis to the 011 interface. Estimates of its interfacial width are about 5.0σ (eight to nine atomic layers) and 4.0σ (six to seven atomic layers) if the derivatives of the energy and Σ function are employed, respectively. As with the 001 face, large structural fluctuations are observed at the 011 interface, as can be seen in Fig. 7. However, the fluctuations here appear primarily in the form of 111 microfacets on the crystal front. These microfacets were observed in all averaged configurations examined for this crystal face (see Fig. 7).

Interfacial widths of 4.8σ (five to six atomic layers) and 3.2σ (three to four atomic layers) are obtained for the 111 interface if the derivatives of the energy and Σ profile functions are utilized, respectively. The magnitude of the structural fluctuations apparent in the 111 solid/liquid interface (see Fig. 8) is much smaller than for the 001 and 011 interfaces. This observation of a reduced structural fluctuation is consistent for all the 111 configurations examined during our analysis.

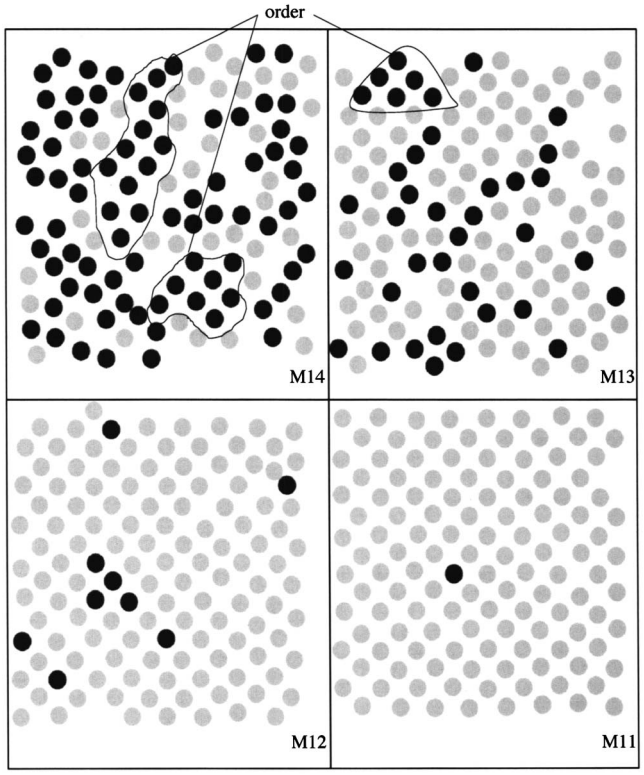

FIG. 6. Averaged configurations of four consecutive slices through the melting interface of the LJ 001 fcc system. The layers are labeled as in Fig. 3. The dark atoms are transient particles as defined in the text. The identified areas show crystalline order.

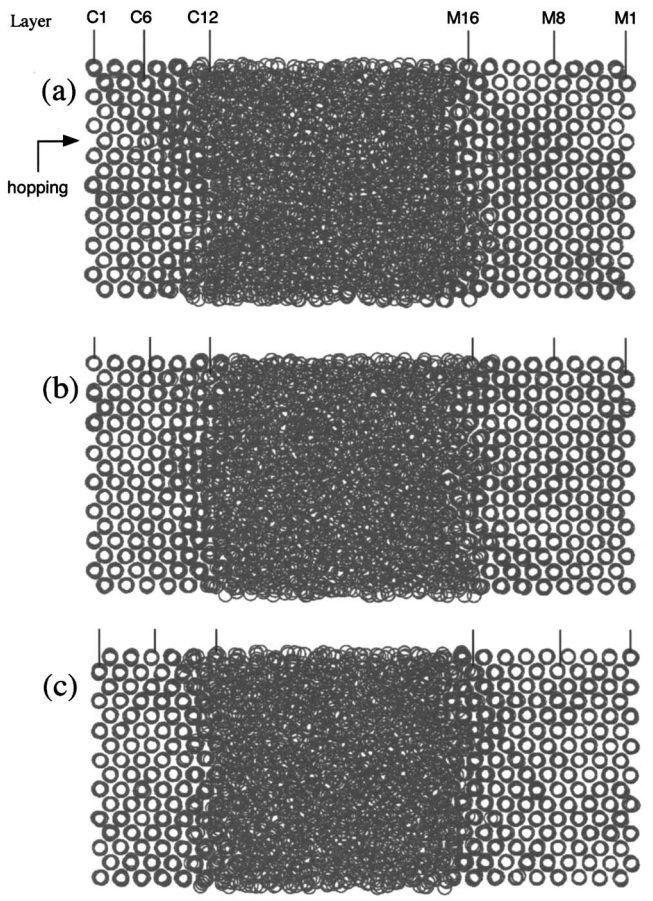

FIG. 7. Three averaged configurations of the LJ 011 fcc depicted in the moving frame. The particles are shown as the open circles and the numbering of the layers are identical to Fig. 2(b); (a) represents an arbitrary initial frame 0, (b) frame 32, and (c) frame 45, where each frame is separated by 750 time steps. The arrow in (a) identifies the row where atom hopping is observed to occur in layer 6.

The extent of the structural fluctuations can be linked to the interfacial tension for each of the various crystal faces, where the magnitude of the structural fluctuations at the interface can be understood[29] as being sensitive to the free-energy cost in forming a unit area of "interface." We observe that the interfacial tension of the 111 crystal face is higher (therefore the free-energy cost of increasing surface area is higher),[23] consistent with the smaller structural fluctuations occurring at this interface.[24] Examining the 001 and 011 faces, their larger fluctuations now reflect the lower free-energy cost in forming a unit area of interface. These faces have been also observed[30] to grow faster than the 111 crystal face. The mechanism of crystal growth for these different faces is bound to their "structural fluctuations," which in turn are determined by their interfacial tensions. The next section will address these outstanding issues.

B. Freezing and melting mechanisms of the 001, 111, and 011 crystal faces

In order to provide a detailed microscopic account of the freezing and melting behaviors for the various crystal faces, we will use information from averaged configurations to illustrate specific characteristics of melting and freezing. The analysis will commence from the liquid side of the interface and move through the center of the interface towards the solid. Generalizations of interfacial behavior on freezing and melting have been made based on extensive observations of steady-state systems. The microscopic dynamics of the particles at the interface is found to be essentially invariant to velocity and gradient. In addition, very recent work[31] examining crystal growth using different thermostating procedures has demonstrated the invariance of the observed behavior at the interface to the detailed microscopic (particle) dynamics.

1. 001 crystal face

The layers C6–C12, as shown in Figs. 2(a), 3(a), and 4, represent the various stages that a slice undergoes during crystallization, as well as capturing the environment influencing the ordering processes. The outermost layer of the crystallizing interface will be examined first. This layer, C12 in Figs. 2(a) and 5, exhibits no obvious atomic layering. At this position, near the liquid edge of the interface, patches of order are just beginning to appear. These patches of order are transient entities, undergoing continuous fluctuations. In layer C11 [see Figs. 2(a) and 5] there is some apparent solidlike behavior, where on average between 0% and 10% of solid order (as defined in Sec. III) is observed and the order here may persist to form a crystalline layer.

At C10 we observe larger solid patches, which tend to persist longer [see Figs. 3 and 5(c)]. We also find large structural fluctuations with between 10% and 50% of solid order in this layer. Inspection of layer C9 reveals that at least half of this slice appears crystalline [see Figs. 2(a), 3, and 4],

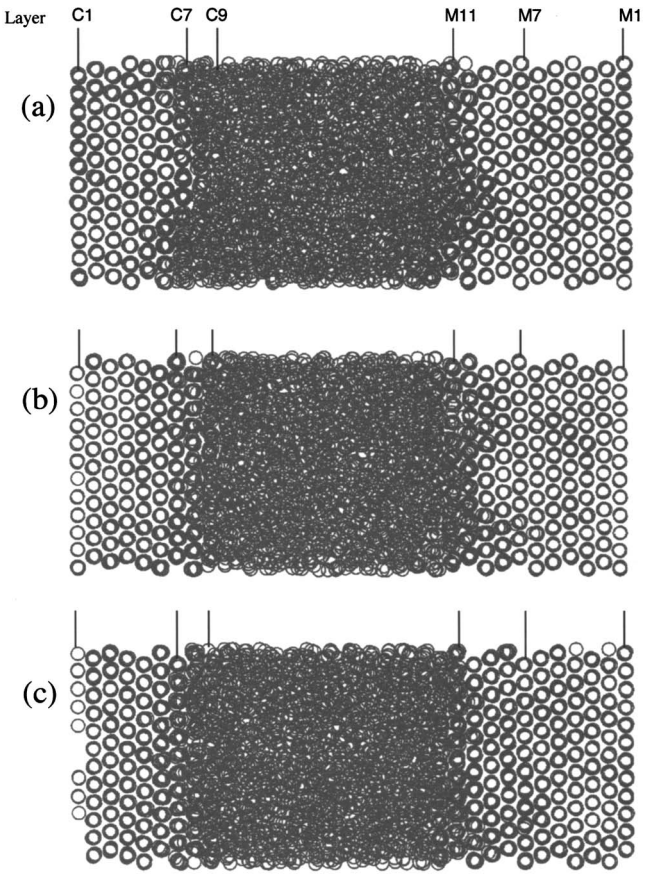

FIG. 8. Three averaged configurations of the LJ 111 fcc depicted in the moving frame. The particles are shown as the open circles and the numbering of the layers are identical to Fig. 2(c); (a) represents an arbitrary initial frame 0, (b) frame 11, and (c) frame 50, where each frame is separated by 750 time steps.

although we sometimes observe [see Fig. 5(a)] considerably less order in this layer. It is clear from Fig. 2(a) that C9 corresponds to the middle of the interface. In Fig. 4, the atoms of layer C9 are labeled black and gray, where the gray (tagged) atoms are those that are still present in the final crystalline layer (as described in Sec. III). Hence, black particles are those atoms that do not end up in the final crystalline layer. Yet Fig. 4 (C9) clearly shows that many of these (black) atoms are in crystalline positions. Such black atoms are thus only transient occupants of crystalline positions, even though the degree of crystalline order in C9 is between 50% and 80%. These (black) atoms will eventually reside in adjacent layers, primarily C10. This hopping, or exchange, of atoms between layers is a critical dynamical feature of the solid/liquid interface.

Inspecting layer C8 in Figs. 3–5 we see that it appears almost completely crystalline with a few defects. However, there are still some transient (black) atoms in crystalline positions, indicating that this layer is not truly crystalline, but will continue to undergo some exchanges of atoms with adjacent layers. Layer C8 also still contains some distortions of its crystal structure with an estimated 80%–100% crystalline order present. Moving now to C7, we see in Fig. 4 that there are still a few transient (black) atoms in what otherwise appears to be a well-ordered crystalline layer. The particle hopping still occurring in C7 almost exclusively involves exchanges with the layer C8 towards the liquid. Examination of layer C6 (see Figs. 2–4) shows no transient (black) atoms in this layer that lies on the solid edge of the interface. This layer is almost fully crystalline with particle hopping occurring only rarely, where such events appear to be triggered by structural distortions in the adjacent (liquid side) layers. Clearly, the present approach of tagging atoms has allowed us to make detailed observations of atom behavior that might otherwise be easily overlooked.

The mechanism by which the 001 face crystallizes can now be discussed in terms of the descriptions given above. As is evident in Fig. 3(b), there are "fingers" of order that extend through the interface, across layers, revealing that the interface is a complex, three-dimensional and dynamically fluctuating entity. It is this behavior, characterized by constant structural fluctuations where atoms collectively take up and leave crystalline positions, that is inherent to the growing interface.

We now turn to the melting process. Utilizing a method of analysis analogous to the crystallizing interface, our discussion of the melting interface begins on the solid side. Figures 2(a) and 3(a) identify the two outer layers, M10 and M11, of the melting interface. Minor distortions of the crystal layer are observed coupled with observations of atomic hopping, as shown in Fig. 6 (M11); these particle exchanges can be seen to be the first stage of melting. The layer M12 exhibits more distortions and defects with more incidences of atom hopping. At the center of the interface (M13) we observe [see Figs. 2(a), 5, and 6] a layer with only partial solid order. But in addition to particles leaving (exchanging) and the further disordering of the layer, we also observe in M13 evidence of particles reorganizing into (new) ordered structures, as shown in Fig. 6. Continuing through the interface the last two layers, M14 and M15, are similar in structure to the first two layers (C10 and C11) of the crystallizing face. In M14 the majority of the remaining crystalline order is accounted for by transient (black) atoms that make up (new) ordered clusters within the melting interface, as can be seen in Fig. 6.

Naively, one could argue that freezing and crystallizing are just opposite processes. This would be consistent with our observation that profile properties (such as width) are the same for the crystallizing and melting interfaces. However, within a crystallizing (or melting) interface we note that two separate and competing processes are operative, namely, ordering and disordering. Therefore, at a melting front, the disordering processes are occurring faster than the ordering processes. Thus, the structure of layer M13 (see Fig. 6) is very similar to that of C9 (see Fig. 4) where both of these layers are at the center of their respective interfaces and contain 50%–80% of solid order.

There also exists a clear asymmetry[17,18] in the freezing and melting rates despite the similarity of the interfaces, with melting occurring more readily than freezing at higher velocities; this can be understood by again comparing the layers C9 (Fig. 4) and M13 (Fig. 6) at the middle of their respective interfaces. They both show evidence of structural fluctuations and comparatively equal content of solidlike and

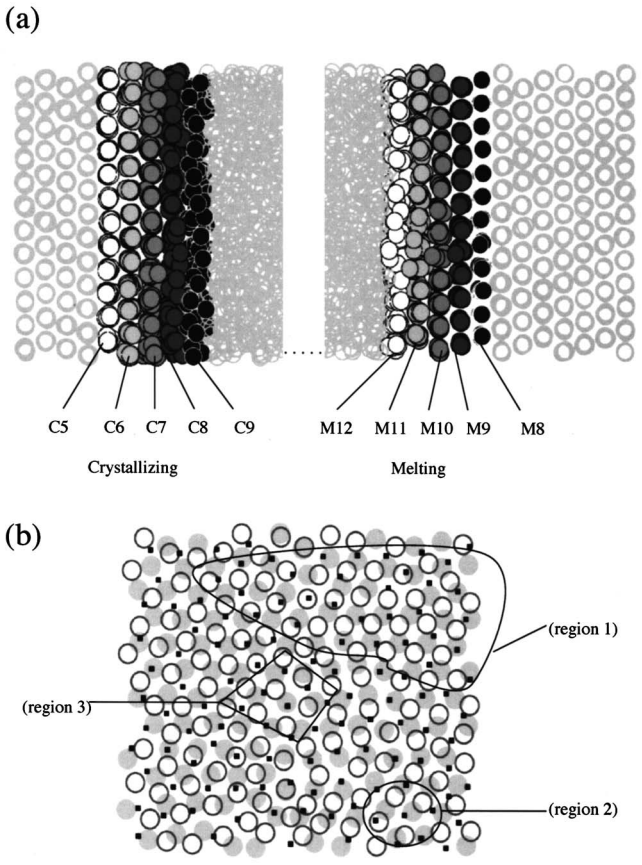

FIG. 9. (a) Layers of the crystallizing (C5–C9) and melting (M12–M8) interfaces of an averaged configuration of a LJ 111 fcc system. Five slices are identified and labeled (shaded differently) for each interface with the layer numbers as given in Fig. 2(c). (b) The forward view of three layers: C9 (small squares), C8 (open circles), and C7 (filled circles). Region 1 shows commensurate crystal structure between C8 and C7. Region 2 contains a hcp cluster and region 3 shows a 001 fcc cluster.

liquidlike behaviors. Within C9, we observe different fragments of several crystal structures, including fcc and some hcp clusters. Consequently, before this layer can crystallize, there needs to be a collective organization of its atoms into a crystalline structure that is commensurate with layer C8. This necessitates that there be sufficient time for the desired structures to appear (as collective fluctuations) and for the undesirable structures to be eventually eliminated. For the melting layer, M13, no such additional time is required, as the defects and mismatched crystal structures will not hinder (and presumably aid) the melting of the layer.

2. 111 crystal face

The crystallization of the 111 interface is examined in Figs. 8–10. The freezing process of the 111 crystal face begins to occur with a few transient patches of order forming in C9 at the liquid edge of the interface (see Fig. 9), which can be either fcc or hcp in nature. These transient patches, also observed by Burke *et al.*,[18] undergo considerable fluctuations and so are similar in behavior to those within the 001 interface. From the averaged configurations shown in Fig. 8, no discernable layer is observable at C9. Moreover, crystal patches have not been observed to persist in C9. At C8 (see Figs. 9 and 10) there appears to be different (competing)

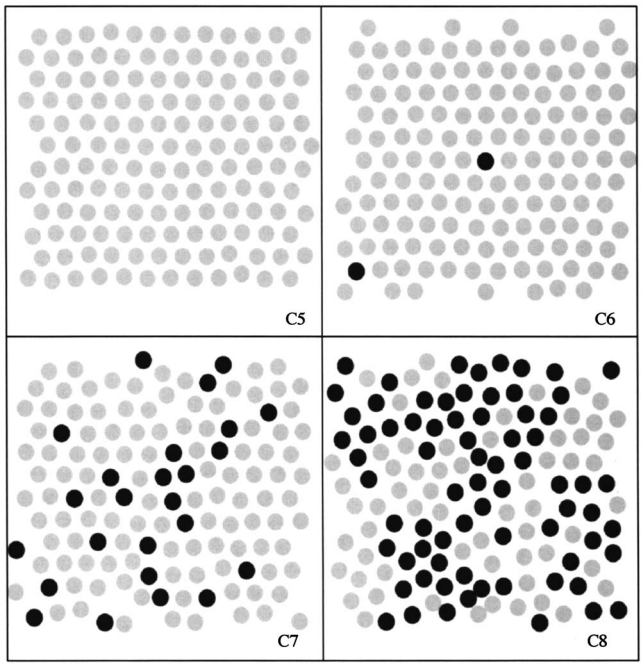

FIG. 10. Averaged configurations of four consecutive slices through the crystallizing interface of the LJ 111 fcc system. The layers are labeled as in Fig. 9. The dark atoms are transient particles as defined in the text.

sublattice structures as a result of structural fluctuations. It is at C8 that the first crystal layer structure is observed, with at least a partial layer evident in Fig. 8(b), but on average only between 10% and 50% solid order is present and none of the crystalline clusters appear to traverse the whole layer. As can be seen in Fig. 10, transient (black) atoms occupy both crystalline (majority) and noncrystalline positions in this layer. In addition, layer C8 was found to influence strongly the solidlike fluctuations of layer C9.

When we inspect C7, slide dislocations and point defects can be found in this layer (see Fig. 10). Figure 8 shows some distortion of the order within this layer, where it is found to exhibit 50%–80% of solid order. We remark that this layer is at the center of the interface. However, exchanges of atoms are still clearly evident between C7 and adjacent layers. C6 as well as C5 appear structurally completely crystalline, yet we still observe particle hopping in these layers. Minor distortions of C6 and C5 are still visually discernable, with the latter, which is now at the solid edge of the interface [see Fig. 2(c)], showing much less distortion.

From Fig. 9(b) one can observe that C8 and C7 have commensurate crystalline order in the area indicated as region 1 and pockets elsewhere. However, we have found that the structural fluctuations that dominate the behavior at C9 are not usually commensurate with C8. In Fig. 9(b) we see that region 2 has a hcp cluster and region 3 a fcc cluster at C9. Therefore, we can identify C9 as the layer with the most apparent dynamic fluctuations, where these fluctuations are sampling many related crystal structures. We also do not observe fingers of order extending through the interface as seen in the 001 interface. Hence, the conclusion here is that the 111 interface is sharper (for example, it has no layer with 0%–10% of solid order) than the 001 interface.

The above analysis suggests that for the 111 face, crystal

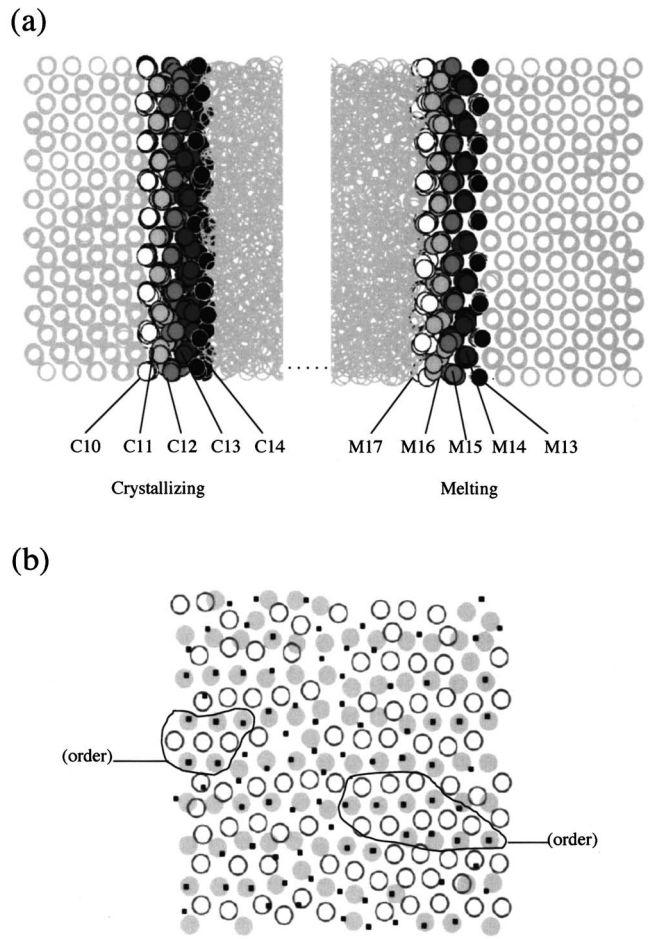

FIG. 11. (a) Layers of the crystallizing (C10–C14) and melting (M17–M13) interfaces of an averaged configuration of a LJ 011 fcc system. Five slices are identified and labeled (shaded differently) for each interface with the layer numbers as given in Fig. 2(b). (b) The forward view of three layers: C14 (small squares), C13 (open circles), and C12 (filled circles). The identified areas exhibit crystalline order.

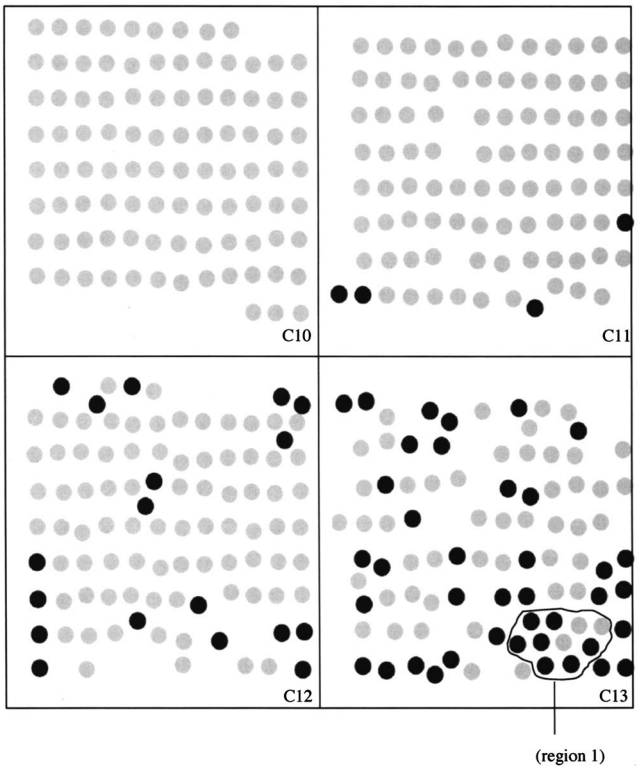

FIG. 12. Averaged configurations of four consecutive slices through the crystallizing interface of the LJ 011 fcc system. The layers are labeled as in Fig. 11. The dark atoms are transient particles as defined in the text. Region 1 shows a hcp cluster.

growth properly begins with layer C8, where it takes considerable time to match correctly the structure within layer C7 (which resides at the center of the interface). This annealing behavior has been seen by Burke *et al.*[18] in their descriptions of crystal growth of the 111 crystal face. However, they did not identify the fluctuation in solid structure within C9, the layer before C8 which is the origin of crystal nuclei that may grow into a crystal layer (only in some cases).

The structure of the 111 melting interface is very similar to that of the 111 crystallizing interface. In essence, the same behavior is observed within layers M8–M12 as was described for C5–C9, but where in the former disordering processes appear to dominate. Not surprisingly then, the melting process for the 111 face is as described for 001, with the same mechanism operative and responsible for the asymmetry between the freezing and melting rates.

3. 011 crystal face

The behavior at the 011 crystal face is in many respects rather similar to that of the 001 interface. Examining layer C14 in Fig. 11 at the liquid edge of the crystallizing interface [see Fig. 2(b)], we find behavior analogous to that seen with the 001 interface with patches exhibiting crystalline character apparent; fcc, hcp, and 011 commensurate structures are observed. Only the latter structures persist and grow if they are commensurate with the underlying crystalline structure. The crystalline order in C14 varies between 0% and 10%. At layer C13 we now find considerably more crystalline character (between 10% and 50%), as shown in Figs. 11(b) and 12. The latter figure also reveals a hcp cluster as indicated. From Fig. 7, evidence of 011 layers is just becoming discernable at C13. At C12 we observe more crystalline order, about 50%–80% as shown in Fig. 12. It is at layer C12, at the center of the interface [see Fig. 2(b)], that clear layers are observed in Fig. 7(b). There are also transient (black) atoms in crystalline positions apparent in C12 in Fig. 12. Inspection of C11 reveals point defects; this layer is 80%–100% crystalline and only a few transient (black) atoms are observed in Fig. 12. Finally, at C10 the layer is essentially crystalline with occasional atom hopping occurring (see Fig. 7 although not evident in Fig. 12). The extent of fluctuations in the 011 interface is similar to that seen in the 001 interface, with atom hopping occurring as far as layer C6 [indicated in Fig. 7(a) with an arrow] due to structural fluctuations.

As is the case of 001, the melting front of a 011 face is similar to its crystallizing face with similar interfacial structure and structural fluctuations [compare M13–M17 to C10–C14 in Fig. 11(a)]. The explanation for the asymmetry for the freezing and melting rates is also analogous to that of the 001 crystal face.

4. Comparison of interfaces

We are now able to provide an explanation for why the values from our two measures of interfacial width are different for the 001, 011, and 111 interfaces. The Σ function measures 2D crystalline order. This function will only be sensitive to order in the *x-y* plane of a crystal layer (at the particular *z*). If particle hopping occurs in a layer (accompanied by another particle hopping to fill the vacancy), the crystal layer will essentially retain its 2D order, and the structural order parameter will thus be rather insensitive to such hopping events (evident in Fig. 2 when comparing the derivatives of the structural order parameter and the energy). The energy function on the other hand is sensitive to the energy changes associated with the disorder in a neighboring layer that must be part of the hopping process at either the crystallizing or melting faces. The importance of particle hopping on the solid side of the interface (although still a rare event) explains the slight asymmetry, noted previously,[17] in the shape of the peak in the derivative of the energy profile function. The consequence of this observation impacts the utility of the Lindemann criteria[32] used to categorize the melting process of a heterogeneous system. Melting as we have described it here begins with particle hopping; consequently, the mean-square displacement criterion employed in the Lindemann procedure may not be adequate to capture the one (or few) particle(s) that hops and may underestimate the initial onset of the melting process.

We have observed hopping within all the interfaces in this work. This behavior has also been observed by Huitema *et al.*,[19] but they did not provide a specific account of the role of these atoms. In addition, they do not describe clearly where the interface is located in their simulation and the extent of hopping in relation to this position during crystal growth and melting. Our observations show that hopping behavior is part of both the freezing and melting phenomena as a disordering process; a fluctuating (defective) layer next to a crystalline layer appears to be a sufficient condition. The overall numbers of these transient atoms diminish as we traverse the interface from the liquid to the solid side, although their relative influence increases. The numbers of transient atoms identified in Figs. 4, 6, 10, and 12 are typical for the present systems. However, it should also be noted that the fraction of transient atoms in a particular layer is dependent upon the growth velocity, the numbers increasing as the velocity decreases. Key to the present study is the characterization of the hopping process, where atom hopping can be understood as originating from thermal motion and fluctuations in the local structural environment at the interface.

It is ultimately the collective behavior of many atoms at the interface that determines whether (net) freezing or melting is observed. The basic mechanism by which freezing occurs at the different crystal faces begins with solidlike structural fluctuations within an otherwise liquid region at the edge of the interface. These ordered clusters are transient entities, however, if they match the underlying crystal structure, they may persist and grow. The ordered structure that finally forms may not necessarily contain all its original atoms as we have identified significant occurrences of particle exchanges. These transient atoms, as we have termed them, can take up clear crystalline positions, however, they are observed ultimately to leave the layer, although the layer (or cluster) may otherwise appear crystalline and even defect free. This behavior indicates that liquidlike characteristics can persist well into the solid side of the interface. The growth at the interface, in general, is not governed by two-dimensional layering, but rather we observe a dynamic three-dimensional ordering process that can subtend several layers, where the ordered structure can extend to the edge of the interface. These protrusions of order can extend from a true crystalline layer across three to four layers of the interface towards the liquid, as seen in Figs. 3(b) and 11(b) for the 001 and 011 faces, respectively. 001 and 011 are the widest interfaces, where the former is slightly wider. The crystallizing process is faster for 001 than for the 011 crystal face as the latter appears to sample fcc and hcp structures (in addition to 011 features) which need to be eliminated before a complete layer can be formed. However, as mentioned previously,[17] lower interfacial tension and wider interfaces allow the 001 and 011 interfaces to grow faster than the 111 crystal face. In contrast, less pronounced protrusions or more confined structural fluctuations within the 111 interface, due to its higher interfacial tension, contribute (in addition to the annealing of different crystal types) to the slower growth of the 111 crystal face.

V. CONCLUSIONS

In this paper we have analyzed the atomic-level detail of steady-state crystal growth of LJ systems. Steady-state crystallization was achieved by utilizing a recently developed[17] procedure (employing a moving temperature gradient) to induce crystal growth. Use of the derivatives of the energy and structural order-parameter profile functions enabled us to obtain the position and the width of the interface. To facilitate our analysis of the interfacial detail of the atomic systems under investigation, averaging procedures for atomic coordinates were employed to remove effectively all thermal motion, thereby capturing the essential translational motion associated with the steady-state freezing or melting processes. Subsequently, derivatives of the corresponding profile functions were superimposed on the resulting averaged configurations to help identify the interfacial atomic layers of the systems.

Interfacial widths of 5.2σ, 5.0σ, and 4.8σ were obtained for the 001, 011, and 111 systems, respectively, in agreement with our previous work.[17] In general these interfaces are not planar but rather are rough structures. For a particular crystal face the structure of the freezing and melting interfaces was found to be very similar, with the layer identified at the center of both showing 50%–80% solid structure. We find that these interfaces are fluctuating entities, with competing ordering and disordering processes occurring at both freezing and melting interfaces; the process that dominates (determining if either net crystal growth or melting is observed) is thus dependent on the conditions at the interface. The structural fluctuations that dominate the behavior at the interface can be either solidlike or liquidlike. Due to these fluctuations the interface is not well delimited and clearly defined sites (to

which atoms can attach themselves) cannot be identified. Instead we observe significant cooperative behavior within clusters (or patches) of atoms. Moreover, we find considerable atomic hopping between layers at both the freezing and melting interfaces; this atomic behavior introduces liquidlike characteristics primarily into the solid side of the interface. Based on our observations, we could also describe the interface as consisting of a center, a solid region with liquidlike structural fluctuations and a liquid region with solidlike structural fluctuations.

The structural fluctuations within the 001 and 011 interfaces are more pronounced than those apparent in the 111 face. These fluctuations, which help facilitate the faster growth of the 001 and 011 faces, introduce three-dimensional crystalline "fingers" through the interface, extending as far as three or four atomic layers. In contrast, the 111 crystal interface is a narrower interface where fingers of order extend at most to two layers.

Since the observed growth rate is the result of the competing ordering and disordering processes at the solid/liquid interface, near equilibrium no discontinuous behavior in the rate can be expected. The asymmetry in the freezing and melting rates apparent at higher rates for the three crystal faces can be understood by examining the layer at the center of the interfaces. Under conditions of crystal growth, this layer can be thought of as consisting of ordered clusters that are not necessarily commensurate with the structure of the underlying crystal and annealing must take place for growth to proceed; such processes will require a critical amount of time. However, for the melting process no such annealing is required and, in fact, the presence of defects should aid in the melting. Consequently, the asymmetry becomes more pronounced at higher growth rates as expected.

In conclusion, we have provided a clear and unambiguous means of describing and defining the detailed atomic structure of the solid/liquid interface. Moreover, we have shown how the processes of crystallizing and melting occur at the atomic level and how the properties of the interface directly influence the behavior of the different crystal faces of atomic systems. The application of the present methodology to molecular systems, such as the ice/water interface, will be examined in forthcoming articles.[33–35]

ACKNOWLEDGMENT

We are grateful for the financial support of the Natural Sciences and Engineering Research Council of Canada.

[1] J. Lyklema, *Fundamentals of Interface and Colloid Science*, Solid-Liquid Interfaces, Vol. II (Academic, London, 1995).
[2] D. P. Woodruff, *The Solid-Liquid Interface* (Cambridge University Press, London, 1973).
[3] I. Benjamin, Annu. Rev. Phys. Chem. **48**, 407 (1997).
[4] *The Solid-Gas Interface*, edited by E. A. Flood (Marcel Dekker, New York, 1967), Vols. I and II.
[5] *Handbook of Surfaces and Interfaces*, edited by L. Dobrzynski (Garland STPM, New York, 1979), Vols. I and II.
[6] C. D. Stanners, D. Gardin, and G. A. Somorjai, J. Electrochem. Soc. **141**, 3278 (1994).
[7] Y. K. Tovbin, Prog. Surf. Sci. **34**, 1 (1990).
[8] M. A. van Hove, Surf. Interface Anal. **28**, 36 (1999).
[9] J. Stangl, V. Holy, and G. Bauer, Rev. Mod. Phys. **76**, 725 (2004); P. Moriarty, Rep. Prog. Phys. **64**, 297 (2001).
[10] M. Plischke and B. Bergersen, *Equilibrium Statistical Physics* (World Scientific, Singapore, 1999).
[11] M. Asta, F. Spaepen, and J. F. van der Veen, Mater. Res. Bull. **29**, 920 (2004).
[12] E. Johnson, Science **296**, 477 (2002); J. M. Howe, *Interfaces in Materials* (Wiley, New York, 1997).
[13] *X-ray Spectrometry: Recent Technological Advances*, edited by K. Tsuji, J. Injuk, and R. van Grieken (Wiley, West Sussex, England, 2004).
[14] J. M. Howe and H. Saka, Mater. Res. Bull. **29**, 920 (2004); J. F. van der Veen and H. Reichert, *ibid.* **29**, 958 (2004).
[15] B. B. Laird and A. D. J. Haymet, Chem. Rev. (Washington, D.C.) **92**, 1819 (1992).
[16] K. A. Jackson, J. Cryst. Growth **198/199**, 1 (1999).
[17] M. S. Gulam Razul, E. V. Tam, M. E. Lam, P. Linden, and P. G. Kusalik, Mol. Phys. **103**, 1929 (2005).
[18] E. Burke, J. Q. Broughton, and G. H. Gilmer, J. Chem. Phys. **89**, 1030 (1988).
[19] H. E. A. Huitema, M. J. Vlot, and J. P. van der Eerden, J. Chem. Phys. **111**, 4714 (1999).
[20] J. Q. Broughton and G. H. Gilmer, J. Chem. Phys. **84**, 5759 (1986).
[21] R. L. Davidchack and B. B. Laird, J. Chem. Phys. **118**, 7651 (2003).
[22] J. R. Morris and X. Song, J. Chem. Phys. **119**, 3920 (2003).
[23] A. William, R. Moss, and P. Harrowell, J. Chem. Phys. **99**, 3998 (1993).
[24] J. Q. Broughton, A. Bonissent, and F. F. Abraham, J. Chem. Phys. **74**, 4029 (1981).
[25] J. Q. Broughton and G. H. Gilmer, J. Chem. Phys. **84**, 5749 (1986).
[26] J. A. Hayward and A. D. J. Haymet, J. Chem. Phys. **114**, 3713 (2001).
[27] O. J. Lanning, S. Shellswell, and P. A. Madden, Mol. Phys. **102**, 839 (2004).
[28] R. Moss and P. Harrowell, J. Chem. Phys. **101**, 9894 (1994).
[29] D. Chandler, *Introduction to Modern Statistical Mechanics* (Oxford University Press, New York, 1987), p. 47.
[30] J. Q. Broughton, G. H. Gilmer, and K. A. Jackson, Phys. Rev. Lett. **49**, 1496 (1982).
[31] D. Cyr and P. G. Kusalik (unpublished).
[32] F. A. Lindemann, Phys. Z. **11**, 609 (1910).
[33] M. S. Gulam Razul, J. G. Hendry, L. Hernández de la Peña, and P. G. Kusalik, Nature (London) (submitted).
[34] M. S. Gulam Razul and P. G. Kusalik (unpublished).
[35] M. S. Gulam Razul, J. G. Hendry, and P. G. Kusalik (unpublished).